Isotopic Yields From the Projectile Fragmentation of ^{20}F, ^{20}Ne, ^{20}Na + Au at 32 MeV/nucleon

D.J. Rowland, E. Ramakrishnan[a], R. Laforest[b], E. Martin,
A. Ruangma, E.M. Winchester, S.J. Yennello

[a] *Microcal Software, Inc., One Roundhouse Plaza, Northampton, MA 01060*
[b] *Mallinckrodt Institute of Radiology, 510 S. Kingshighway, St. Louis, MO 63110*

In the last decade there has been a proliferation of studies to probe the multi-fragmentation of excited nuclear matter. In order to study this phenomenon, research has been performed using a wide range of projectile energies and projectile/target combinations to study the mechanisms leading to fragmentation. The goal of these investigations has been to understand excited nuclear matter and the fragmentation process in terms of the nuclear equation of state.

The reactions under investigation here are ^{20}F, ^{20}Ne, ^{20}Na + Au at 32 MeV/nucleon. The reactions were performed at the Texas A&M University Cyclotron Institute using the FAUST detector array [1]. The radioactive beams were produced and isolated with the MARS beamline [2]. Projectile fragments were identified in the FAUST array that consists of 68 Si/CsI telescopes covering 90% of the solid angle in the region from 2.31° to 33.63°. Isotopic identification for hydrogen and helium was possible for all detectors and up to Z=7 for nearly half of the detectors.

Event selection was performed in such a manner as to isolate the fragmenting projectile and exclude any particles emanating from the target nucleus. This was done by plotting the sum of the collected charge versus the sum of the parallel momentum for events with multiplicity two or greater. Reconstructed projectile events are those where the summed charge is equal to the beam Z and the reconstructed momentum is within a defined range. The cut on momentum is determined by projecting the momentum for the reconstructed beam charge onto the parallel momentum axis. A Gaussian was fit to the distribution and the momentum cut was chosen to be within 3σ of the mean. For the data presented in this report, isotopic identification was only performed up to boron.

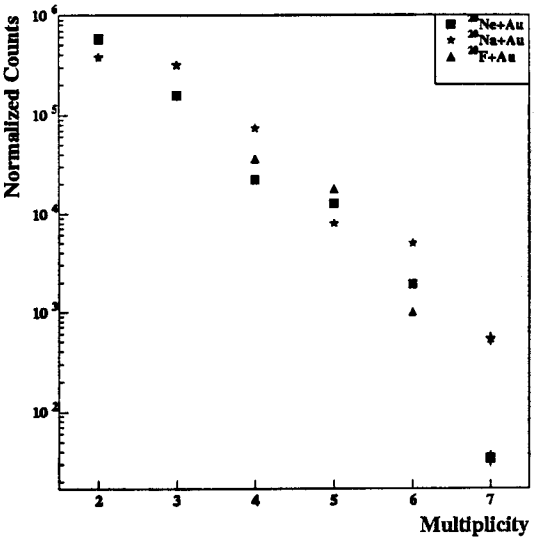

Figure 1. Charged particle multiplicity distribution for the three reactions. The ^{20}F and ^{20}Na reactions are normalized to the total counts for the ^{20}Ne reaction. The ^{20}F data for multiplicity 1, 2, and 7 overlap with the ^{20}Ne data. Statistical error bars are plotted and are smaller than the size of the markers.

A comparison of the ^{20}F, ^{20}Ne, ^{20}Na + Au is shown in Figures one to three for some basic observables. For Figures one and two the ^{20}F and ^{20}Na distributions have been normalized to the total number of accepted events for the ^{20}Ne distribution. Error bars for the three

figures are statistical. Figure one shows the charged particle multiplicity distributions for the three reactions. As the neutron content is decreased the slope of the multiplicity distribution begins to flatten. This is possibly due to a combination of two factors. The flattening may be a result of the Coulomb contribution to the fragmentation of the projectile. Also, due to the low Z of the nuclei under investigation, more exit channels at higher multiplicity are possible for the beams with higher Z. This difference in the number of possible exit channels for the different beams may also account for the large difference in counts at the highest multiplicity.

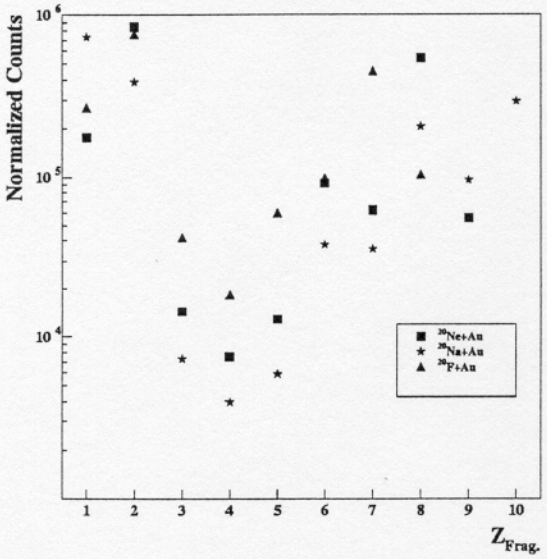

Figure 2. Charge particle distribution for the three reactions. The ^{20}F and ^{20}Na reactions are normalized to the total counts for the ^{20}Ne reaction. Statistical error bars are plotted and are smaller than the size of the markers.

Figure two shows the charged particle distribution. Note the asymmetry in the distribution of emitted charged particles, however, as the neutron content of the projectile is increased the asymmetry begins to flatten. It is also clear that the ^{20}Na beam produces a lot of Z=1. This may account for similar shapes in the ^{20}Na and ^{20}Ne charged particle distributions between Z=2 and Z=8 because the Na loses a particle with Z=1 and then breakups up like a lighter isotope of Ne.

The average neutron to proton ratio is shown in Figure three. The ratio is defined for Z=1 in the inset of the figure. ^{1}H, ^{2}H and ^{3}H are summed for the total number of counts for the given reaction. The plot shows a large odd even effect for the ^{20}Na data. Like the flattening of the charged particle distribution, as the neutron content of the projectile is increase the odd-even effect begins to flatten. A more detailed analysis is currently underway.

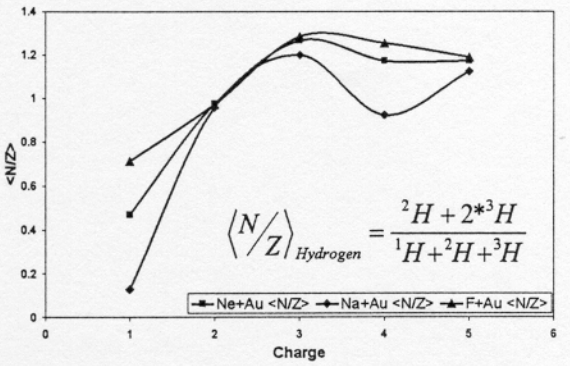

Figure 3. Average neutron to proton ratio for the three reactions. The neutron to proton ratio for Z=1 is defined by the inset equation. Statistical error bars are plotted and are smaller than the size of the markers.

References

[1] F. Gimeno-Nogues, *et al.*, Nucl. Inst. and Meth. in Phys. Res. A **399**, 94(1997).

[2] R.E. Tribble, *et al.*, Nucl. Inst. and Meth. in Phys. Res. A **285**, 441(1989).